Adsorption of Carbon Dioxide and Methane on Cobalt Gallate-Based Metal-Organic Framework (Co-Gallate): Equilibrium Isotherm, Thermodynamic and Kinetic Studies

Marhaina Ismail[1], Mohamad Azmi Bustam[2,*], Yin Fong Yeong[1]

[1] Carbon Dioxide Research Centre (CO₂RES), Universiti Teknologi PETRONAS, Bandar Seri Iskandar 32610, Perak, Malaysia
[2] Centre of Research in Ionic Liquids (CORIL), Universiti Teknologi PETRONAS, Bandar Seri Iskandar 32610, Perak, Malaysia

ARTICLE INFO	ABSTRACT
	Biogas is mainly consisted of methane and carbon dioxide in the presence of other contaminants. The biogas purification by adsorption using metal-organic frameworks is getting attention due to the low-cost operation and high-efficiency process. Co-gallate was predicted to give a promising performance in CO_2 and CH_4 adsorption. However, the behaviours of CO_2 and CH_4 adsorption on Co-gallate are not well-explained. Therefore, this work is to synthesize Co-gallate and its performance was discussed in terms of adsorbed amount of CO_2 and CH_4. The experimental CO_2 and CH_4 pure adsorption isotherms were then fitted with equilibrium isotherm and kinetic models to describe the adsorption behaviours. Co-gallate offered a greater CO_2 adsorption capacity than CH_4 due to a stronger adsorbent-adsorbate interaction. The experimental pure adsorption isotherms were best fitted with Toth model compared to Langmuir, Freundlich and Sips models according to the R^2 values. Toth model described the CO_2 adsorption was multilayer and heterogeneous. Thermodynamic property suggested the CO_2 and CH_4 adsorption were classified as exothermic process and physisorption. For kinetic models, pseudo-first order model brought the highest goodness-of-fit in terms of rate of adsorption compared to pseudo-second order and Elovich models. Pseudo-first order model reflects the adsorption rate is proportional to the number of vacant sites. It confirmed CO_2 adsorption was more favourable than CH_4, at lower temperature condition. In this work, the equilibrium isotherm and kinetic models were employed to select the best-fitted model in explaining the adsorption behaviours. Therefore, these behaviours of CO_2 and CH_4 adsorption on Co-gallate are useful in designing the future practical operation of CO_2/CH_4 gas adsorption.

1. Introduction

The renewable energies are very important in order to save the planet and can bring the positive economic impacts. They can help to reduce the global warming and greenhouse effects as these issues rise from the human activities such as combustion of coal, oil and natural gas [1]. Biogas is a

natural occurrence and classified as one of the renewable sources of energy. The usage of biogas can reduce the release of methane to the atmosphere and lessen the reliability on fossil fuels [2]. Biogas is typically generated through anaerobic degradation of biomass by microorganisms by decomposing the organic compounds in the absence of oxygen [3]. The sources of biogas normally come from industrial wastewater, landfills, household wastes as well as animal and crop wastes in which the composition of biogas produced at atmospheric pressure can be varied based on the biomass sources [4]. Biogas is mainly consisted of 50-70 % of methane, 30-50 % of carbon dioxide and other contaminants such as hydrogen sulphide, carbon monoxide, hydrogen, water vapor, and so on [5]. Heat and electricity can be produced since the raw biogas can provide a high calorific content between 5000-7000 kcal/m^3 [6]. The raw biogas needs to be purified (CO_2 removal) in order to enhance the heating values and to avoid corrosion in the equipment's and pipelines before it can be transported, stored and used. The purified and upgraded biogas typically can reach above 96 % CH_4 content [3].

The methods for biogas purification/upgrading such as solvent absorption, membrane and cryogenic are uneconomic intensive due to the high cost and energy consumptions. Adsorption using solid adsorbents becomes progressively competitive because it can offer a low cost and energy effective process. It is a surface occurrence occurs when the adsorbates attach on the surface of solid adsorbents. The main state-of-art for adsorption is the solid adsorbents. The conventional adsorbent materials such as activated carbon, graphene oxide nanocomposite and even agricultural waste like palm kernel shell are commonly used in variety of adsorption processes [7-10]. Nowadays, metal-organic frameworks (MOFs) which are defined as hybrid porous compounds consist of organic linkers and inorganic moieties, are getting attention because of their exclusive properties such as excellent structural designability and pore tunabililty. Therefore, MOFs can be designed and tailored to accomplish on-demand targeted applications.

To enhance the biogas purification, more attention should be given on two main factors which are the capability of solid adsorbents and effectiveness of the process design [11]. Gallate-based metal-organic frameworks or known as M-gallate were proven can act as the new solid adsorbents for CO_2 and CH_4 separation based on the prediction done by the previous work [12]. The prediction results showed cobalt gallate-based MOF (Co-gallate) is one of the promising adsorbent among the studied gallate-based MOFs. Nevertheless, to date there has been no report on the equilibrium isotherm, thermodynamic and kinetic studies of CO_2 and CH_4 adsorption using Co-gallate. These parameters are very important to provide the valuable information for designing adsorption and separation process.

Therefore, this work is about the synthesis of Co-gallate to be subjected for the pure gas adsorption of CO_2 and CH_4. The experimental CO_2 and CH_4 pure adsorption isotherms were discussed in terms of adsorption capacity (adsorbed amount). Then, the experimental isotherms were fitted to equilibrium isotherm models such as Langmuir, Freundlich, Sips and Toth models. The best-fitted model constant values were used to determine the thermodynamic properties. Lastly, the experimental data were explained in terms of kinetic models namely pseudo-first order, pseudo-second order and Elovich models. The equilibrium isotherm and kinetic models are well-known approach in describing the adsorption behaviours. These equilibrium isotherm, thermodynamic and kinetic studies are expected to bring a beneficial information for designing the practical application of CO_2/CH_4 adsorption using Co-gallate.

2. Methodology

2.1 Materials

Cobalt (II) chloride anhydrous, $CoCl_2$ (98 %), gallic acid anhydrous, $C_7H_6O_5$ (98 %), potassium hydroxide, KOH (85 %), and ethanol absolute, C_2H_5OH (99.8 %) were purchased from Merck without any further purification. CO_2 (99.99 %) and CH_4 (99.995 %) purified grade gas tanks were supplied by Linde Malaysia.

2.2 Synthesis of Co-Gallate

Co-gallate was synthesized by hydrothermal synthesis method [13]. $CoCl_2$ (0.05 mol) and gallic acid (0.1 mol) were mixed with 0.25 L of KOH aqueous solution (0.16 M) in a round-bottomed flask. Under a reflux condition at ambient pressure, the mixture was heated at 353 K with a non-stop stirring for 24 hours. Then, the mother liquor was removed to separate the solid product. The solid product was washed by using deionized water before been immersed in ethanol. The ethanol was replenished twice for two days. The solid product was undergone characterization analysis including the Powder X-ray Diffraction (PXRD), Fourier Transform Infrared Spectroscopy (FTIR) and Surface Area and Porosity (SAP). The detailed explanation of the characterization analysis can be found from the previous work [14].

2.3 CO_2 and CH_4 Pure Gas Adsorption

The adsorption of pure CO_2 and CH_4 gases were recorded using 3FLEX Micromeritics Surface Characterization at 273, 298 and 313 K and up to 1 bar. Co-gallate was degassed/activated under vacuumed condition for 24 hours at 393 K before the measurement.

2.4 Equilibrium Isotherm Models

The experimental CO_2 and CH_4 pure adsorption isotherms at 273, 298 and 313 K were fitted with four well-known models namely Langmuir, Freundlich, Sips and Toth models. Table 1 shows the general equation of respective models with their corresponding linear forms. The detailed explanation on the studied isotherm models can be found based on the previous works as stated in Table 1.

Table 1
Equilibrium isotherm models

Model	General Form	Linear Form	Reference
Langmuir	$q_e = \frac{q_m K_L P_e}{1 + K_L P_e}$	$\frac{P_e}{q_e} = \frac{P_e}{q_m} + \frac{1}{K_L q_m}$	[15,16]
Freundlich	$q_e = K_F P_e^{1/n}$	$\log q_e = \log K_F + \frac{1}{n} \log P_e$	[16,17]
Sips	$q_e = \frac{q_m (K_S P_e)^{1/n}}{1 + (K_S P_e)^{1/n}}$	$\ln\left(\frac{q_e}{q_m - q_e}\right) = \frac{1}{n} \ln P_e + \ln\left(K_S^{1/n}\right)$	[16,18,19]
Toth	$q_e = \frac{q_m K_T P_e}{[1 + (K_T P_e)^n]^{1/n}}$	$\ln\left(\frac{q_e^n}{q_m^n - q_e^n}\right) = n \ln P_e + n \ln K_T$	[20-22]

where q_e and q_m (mmol/g) signify the gas adsorbed amount over adsorbent mass at equilibrium and maximum adsorption capacity respectively, P_e (mbar) is the equilibrium pressure, and n (dimensionless) is the heterogeneity factor. K_L, K_F, K_S and K_T (1/mbar) are the constants of Langmuir, Freundlich, Sips and Toth models respectively.

The obtained equilibrium isotherm model constants could determine thermodynamic properties using van Hoff's formulation as stated below [23]:

$$\Delta G° = -RT \ln k_{eq} \tag{1}$$

$$\Delta G° = \Delta H° - T.\Delta S° \tag{2}$$

where k_{eq} is the equilibrium isotherm model constant in which the linear plot of $\ln k_{eq}$ versus $1/T$ can determine the values of $\Delta S°$ and $\Delta H°$, indicate by the y-intercept and slope respectively. T (K) is temperature and the universal gas constant is denoted by R (8.314 J/mol.K).

2.5 Kinetic Models

The studied kinetic models in this work included pseudo-first order, pseudo-second order and Elovich models. The general and linearized form of the kinetic models were simplified in Table 2. The detailed description on the studied kinetic models were explained based on reported literatures as stated in Table 2.

Table 2
Kinetic models

Model	General Form	Linear Form	Reference
Pseudo-first order	$q_t = q_e(1 - e^{-k_f t})$	$\log(q_e - q_t) = \log(q_e) - (\frac{k_f}{2.303})t$	[24,25]
Pseudo-second order	$q_t = \frac{q_e^2 k_s t}{1 + q_e k_s t}$	$\frac{t}{q_t} = \frac{t}{q_e} + \frac{1}{k_s q_e^2}$	[25,26]
Elovich	$q_t = \frac{1}{\beta}\ln(1 + \alpha\beta t)$	$q_t = \frac{1}{\beta}\ln(\alpha\beta) + \frac{1}{\beta}\ln t$	[23,27]

where t is time, q_e and q_t (mmol/g) are the adsorption capacities (adsorbed amount) at equilibrium and a given time respectively. k_f (min⁻¹) is the pseudo-first order rate constant and k_s (g/mmol.min) is the pseudo-second order rate constant. α is the initial adsorption rate constant (mmol/g.min) and β (g/mmol) is the extent of the surface coverage and related to activation energy of the adsorption.

The obtained adsorption rate constant could determine activation energy (E_a) using Arrhenius equation as shown below [28]:

$$k = Ae^{-(\frac{E_a}{RT})} \tag{3}$$

where E_a (J/mol) is the activation energy, k is the adsorption rate constant and the pre-exponential factor is designated by A.

3. Results
3.1 Characterization of Co-Gallate
3.1.1 Powder x-ray diffraction (PXRD) pattern

The crystallinity of Co-gallate was examined and its PXRD pattern is presented in Figure 1.
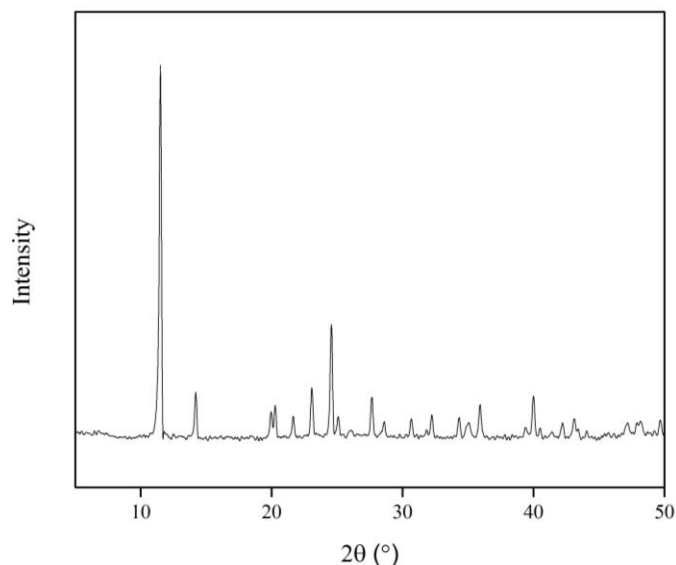
Fig. 1. PXRD pattern of Co-gallate

The nature of crystallinity of Co-gallate could be identified by the sharp peaks and it disclosed three substantial diffraction peaks at 11.53°, 14.15° and 24.53°. The average crystalline size of Co-gallate was 47.6 nm, calculated by using Debye-Scherrer equation [29]. It is worth to note the crystalline size calculated by the Debye-Scherrer equation is not necessarily corresponded to the particle size [30].

3.1.2 Fourier transform infrared spectroscopy (FTIR) spectrum

Figure 2 displays FTIR spectrum of Co-gallate to investigate the functional groups of crystalline adsorbent.
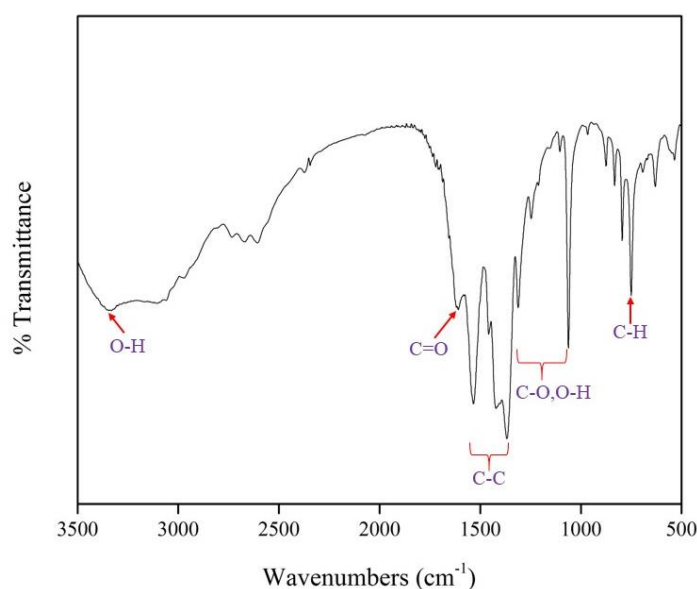
Fig. 2. FTIR spectrum of Co-gallate

The functional groups of Co-gallate are described in Table 3.

Table 3
Description of FTIR spectrum of Co-gallate

Wavenumber (cm^{-1})	Description
3500-2800	A strong and broad band represented the stretching vibration of O-H of a carboxyl group.
1610	A narrow peak attributed a carbonyl (C=O), which indicated the presence of carboxyl group.
1528, 1424, 1372	These three peaks were typical stretching vibrations of C-C bonds in an aromatic ring of gallic acid.
1300-1000	A few peaks in this region signified the stretching vibrations of C-O bond and the bending vibration of O-H bond of the aromatic ring.
749	This sharp peak showed the C-H bond of the aromatic ring.

Therefore, the functional groups of Co-gallate were acknowledged based on the descriptions of IR spectrum and well-agreed with the literature [29].

3.1.3 Porous properties

Nitrogen (N_2) adsorption and desorption isotherms and BJH pore size distribution of Co-gallate are displayed in Figure 3. It shows a very large hysteresis existed due to the occurrence of capillary condensation.

(a)   (b)
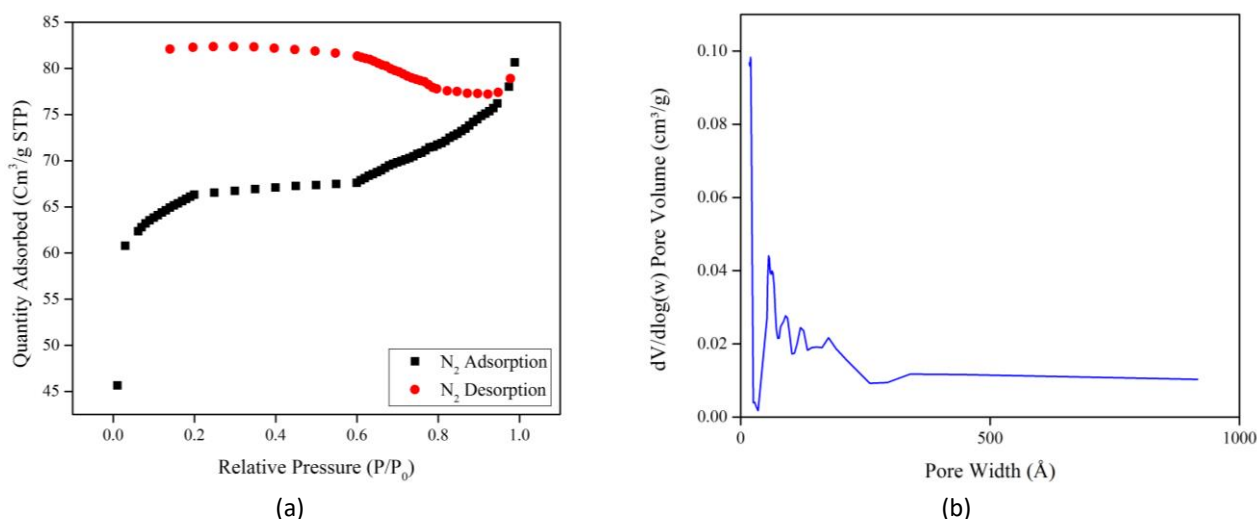
Fig. 3. (a) N_2 adsorption-desorption isotherms and (b) BJH pore size distribution of Co-gallate

The Brunauer-Emmett-Teller (BET) method was applied to the N_2 isotherm at the relative pressure between 0.00-0.13 to calculate the BET surface area. The BET surface area of Co-gallate was calculated to be 248.4 m^2/g. By using t-plot method, the pore volume was estimated to be 0.10 cm^3/g. The mean pore size of Co-gallate was found to be 4.93 nm, determined by using Barrett-Joyner-Halenda (BJH) model.

3.2 CO_2 and CH_4 Pure Adsorption Isotherms

The experimental CO_2 and CH_4 pure adsorption isotherms for Co-gallate are plotted as shown in Figure 4. CO_2 pure adsorption isotherms reflected S-shaped curves in which the knee-shaped section was more obviously seen as temperature increased. Meanwhile, CH_4 pure adsorption isotherms reflected to linear isotherm.

Based on Figure 4, the adsorbed amount of both CO_2 and CH_4 gases increased with the pressure. In adsorption, the stronger adsorption sites were occupied first and the availability of active sites were gradually decreased, resulted in the maximum adsorbed amount when they reached saturation. Meanwhile, the adsorbed amount of CH_4 did not approach the saturation state even at the highest pressure considered in this work. The CO_2 adsorption capacity values were greater than CH_4 at all studied temperature. At 1 bar condition, the CO_2 adsorption capacity was intended to be 4.38, 3.63 and 2.29 mmol/g, while CH_4 offered 0.365, 0.233 and 0.143 mmol/g at 273, 298 and 313 K respectively. This is mainly because CO_2 has a greater quadrupole moment while CH_4 has none, resulted in a stronger electrostatic interaction between CO_2 molecules and Co-gallate [31]. It means the affinity between CO_2 and Co-gallate was stronger and favorable which led to a greater CO_2 adsorption capacity.
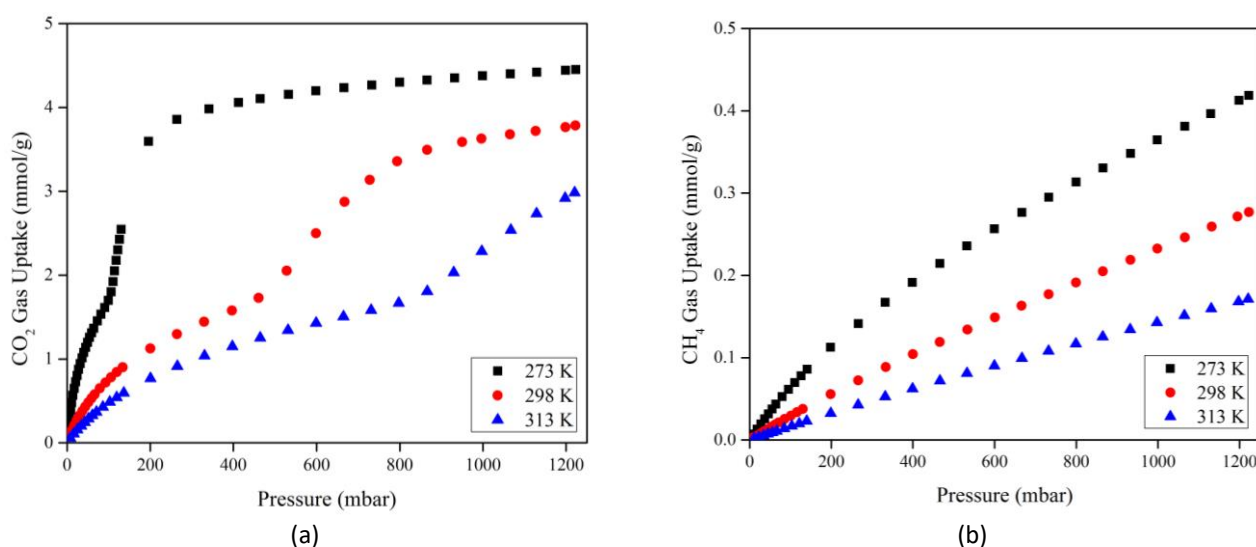
Fig. 4. (a) CO_2 and (b) CH_4 pure adsorption isotherms of Co-gallate at 273- 313 K

In terms of temperature, the adsorbed amount of CO_2 and CH_4 decreased as temperature increased since adsorption is classified as exothermic process. A higher temperature affected the surface adsorption energy and molecular diffusion rate to escalate, initiating the gas molecules become unsteadily moving and hinder from being attached onto the surface of adsorbent, leading to decrement of the adsorbed amount [32]. Subsequently, a higher temperature condition may reduce the adsorbed amount since it is not advantageous for adsorption process.

3.3 Equilibrium Isotherm Models

The mechanism and adsorption data interpretation can be done by using either a theoretical or empirical equation since the adsorption isotherms correspond to the adsorbent-adsorbate interaction [33]. Equilibrium isotherm models can offer the valuable information in predicting the adsorption behaviours of gas molecules on the adsorbent over an extensive range of temperature and pressure. After applying several equilibrium isotherm models, Toth model was summed up to fit the experimental CO_2 and CH_4 pure adsorption isotherms the best compared to Langmuir, Freundlich and Sips models based on R^2 value as tabulated in Table 4.

Table 4
Equilibrium isotherm model parameters

Model	Parameter	CO$_2$			CH$_4$		
		273 K	298 K	313 K	273 K	298 K	313 K
Langmuir	K_L	7.45 x 10^{-3}	1.64 x 10^{-3}	2.4 x10^{-4}	9.0 x 10^{-4}	3.1 x 10^{-4}	1.7 x 10^{-4}
	q_m	5.0000	5.4915	12.3670	0.7632	0.9680	1.002
	R^2	0.9781	0.9654	0.9698	0.9970	0.9984	0.9992
Freundlich	K_F	0.3153	0.02847	0.01388	1.74 x 10^{-3}	5.1 x 10^{-4}	2.5 x 10^{-4}
	n	2.5602	1.4009	1.3192	1.2809	1.1289	1.0839
	$1/n$	0.3906	0.7138	0.7580	0.7807	0.8858	0.9226
	R^2	0.9128	0.9626	0.9470	0.9944	0.9999	0.9987
Sips	K_S	7.26 x 10^{-3}	3.75 x 10^{-3}	1.31 x 10^{-3}	2.0 x 10^{-4}	1.5 x 10^{-4}	9.0 x 10^{-5}
	q_m	4.8984	4.0362	3.9334	1.8193	1.6706	1.6464
	n	0.8115	0.8375	0.9084	1.1635	1.0360	1.0269
	$1/n$	1.2323	1.1940	1.1008	0.8595	0.9652	0.9738
	R^2	0.9833	0.9069	0.9381	0.9995	0.9997	0.9999
Toth	K_T	5.03 x 10^{-3}	1.25 x 10^{-3}	7.6 x 10^{-4}	1.8 x 10^{-4}	7.3 x 10^{-5}	5.5 x 10^{-5}
	q_m	4.4639	3.8333	3.2205	5.5377	4.5825	3.1526
	n	2.0556	4.7613	11.7925	0.4051	0.5652	0.6873
	R^2	0.9883	0.9800	0.9670	0.9999	0.9996	0.9999

The values of n for CO$_2$ at 273-313 K are greater than unity, resulted in a strong degree of surface heterogeneity compared to CH$_4$. Greater heterogeneity of the adsorbent will enhance the interaction of adsorbent-adsorbate in which it will increase the adsorption capacity. Toth model constants also represented the adsorbent-adsorbate interaction in which the higher the value the greater the affinity, however decreased from 273 to 313 K. As a result, these two parameters contributed to the greater CO$_2$ adsorption capacity compared to CH$_4$. In addition, Toth model develops from Langmuir isotherm which is associated to monolayer and/or multilayer adsorption and applicable for heterogeneous systems [34]. Based on pore size of Co-gallate, it is classified as mesoporous adsorbent according to International Union of Pure and Applied Chemistry (IUPAC) [35]. The mesoporous adsorbent is normally related to Type IV isotherm which is corresponded to multilayer adsorption [35,36]. Therefore, CO$_2$ adsorption can be concluded as multilayer adsorption on heterogeneous surface of Co-gallate.

3.4 Thermodynamic Properties

Thermodynamic properties were determined from the linear plots as presented in Figure 5 and their values are tabulated in Table 5. Equilibrium isotherm model constants (k_{eq}) are Toth model constants at different temperatures since it gave the best-fitted isotherms.
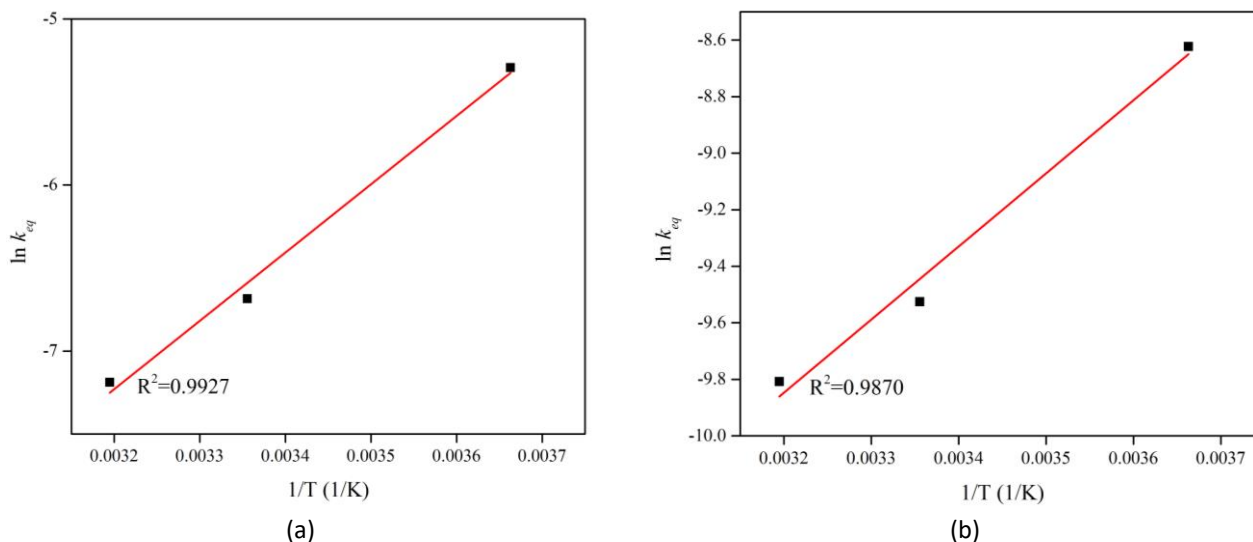
Fig. 5. Van Hoff's plot of (a) CO_2 and (b) CH_4

Based on Table 5, the CO_2 and CH_4 adsorption were classified as exothermic process due to the negative values of change in enthalpy of reaction, $\Delta H°$, in which heat was released throughout the process. In addition, the magnitudes of $\Delta H°$ for CO_2 and CH_4 are -34.21 and -21.50 kJ/mol respectively, reflected the physisorption (physical adsorption) type. The range of $\Delta H°$ for physisorption is found to be 0-40 kJ/mol [37]. The adsorption process could be described to decrease the disorder and randomness at the gas-solid interface based on the negative values of change in entropy, $\Delta S°$. On the other hand, the positive signs of change in Gibbs free energy, $\Delta G°$ indicated the CO_2 and CH_4 adsorption process was non-spontaneous.

Table 5
Thermodynamic properties

Adsorbate	$\Delta H°$ (kJ/mol)	$\Delta S°$ (kJ/mol.K)	$\Delta G°$ (kJ/mol)		
			273 K	298 K	313 K
CO_2	−34.21	−0.17	12.09	16.33	18.87
CH_4	−21.50	−0.15	19.63	23.40	25.66

3.5 Kinetic Models

The correlation between adsorbed amount of CO_2 and CH_4 with time are plotted in Figure 6 to assess the adsorption kinetics.

The pseudo-first order, pseudo-second order and Elovich models were applied to fit the experimental data to determine the reaction rate of adsorption which is important for designing adsorption operation. The kinetic model parameter values are presented in Table 6.

According to the R^2 values, pseudo-first order model offered the highest goodness-of-fit for both CO_2 and CH_4 adsorption at 273-313 K. Pseudo-first order model suggests the adsorption rate is proportional to the number of vacant adsorption sites [38]. As mentioned earlier, the gas molecules would accommodate the stronger adsorption sites first due to the stronger adsorbent-adsorbate interaction, and gradually occupied until it reached saturation. In addition, the pseudo-first order rate constant values, k_f for CO_2 were decreased with temperature, leading to a faster adsorption at lower temperature especially at early stage of adsorption. It can be clarified based on the experimental CO_2 pure adsorption isotherms in which there was a rapid increment of CO_2 uptake at

lower pressure range, however decreased from 273-313 K. Meanwhile, k_f for CH_4 showed a fluctuated trend.

(a)   (b)
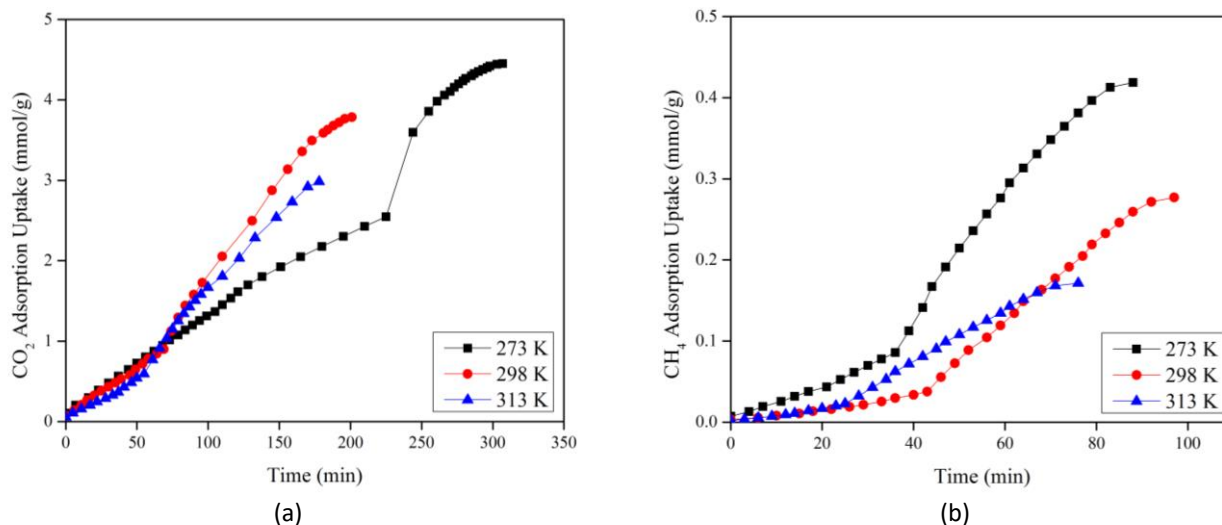
Fig. 6. Adsorbed amount of (a) CO_2 and (b) CH_4 versus time at 273-313 K

Table 6
Kinetic model parameters

Model	Parameter	CO_2			CH_4		
		273 K	298 K	313 K	273 K	298 K	313 K
Pseudo-first order	q_e	4.4055	3.7068	2.9363	0.4130	0.2759	0.1705
	k_f	3.46×10^{-3}	3.34×10^{-3}	3.27×10^{-3}	4.61×10^{-3}	2.53×10^{-3}	4.61×10^{-3}
	R^2	0.9996	0.9967	0.9865	0.9978	0.9962	0.9853
Pseudo-second order	q_e	2.0182	1.3228	1.1330	0.1019	0.0820	0.0397
	k_s	5.72×10^{-3}	0.0130	0.0127	0.3305	0.1335	0.7002
	R^2	0.7831	0.9153	0.6105	0.9071	0.6808	0.6128
Elovich	β	2.9922	4.2230	5.5741	55.249	111.11	178.57
	α	0.0601	0.0553	0.0432	8.08×10^{-3}	2.40×10^{-3}	2.84×10^{-3}
	R^2	0.8987	0.9396	0.8398	0.9527	0.9409	0.8882

3.6 Activation Energy

The pseudo-first order rate constant values were used for the linear plot of Arrhenius equation since it has the highest R^2 values in order to determine the activation energy, E_a. The E_a values were calculated to be -0.97 and -2.15 kJ/mol for CO_2 and CH_4 respectively. The negative values of E_a implied the rate of adsorption decreased with temperatures and more favorable at the lower temperature.

The desorption of CO_2 molecules could be hindered since it has the greater value of E_a than CH_4. It means CO_2 required the higher energy barrier in order to detach from the surface of Co-gallate. On the other hand, a lower value of E_a of CH_4 made the molecules easier to desorb, contributed the lower CH_4 adsorption capacity.

4. Conclusions

The experimental CO_2 pure adsorption isotherm showed the higher adsorption capacity than CH_4 due to stronger affinity between CO_2 molecules and Co-gallate. The experimental CO_2 and CH_4 pure

adsorption isotherms were then fitted with Langmuir, Freundlich, Sips and Toth models. Toth model provided the highest goodness-of-fit in which it confirmed the CO_2 adsorption was multilayer and occurred at heterogeneous surface of Co-gallate. The Toth model constant values were applied to determine the thermodynamic properties in which it verified the adsorption is exothermic process and physisorption. Meanwhile, pseudo-first order model brought the best-fit for CO_2 and CH_4 than pseudo-second order and Elovich models to describe the rate of adsorption. The equilibrium isotherm and kinetic models are systematic approach in explaining the adsorption behaviours. Therefore, these equilibrium isotherm, thermodynamic and kinetic studies are beneficial information in designing the operation of CO_2/CH_4 adsorption system using Co-gallate as the adsorbent.

Acknowledgement

References

[1] Karimi, Mohsen, Alexandre Ferreira, Alírio E. Rodrigues, Farid Nouar, Christian Serre, and José AC Silva. "MIL-160 (Al) as a candidate for biogas upgrading and CO2 capture by adsorption processes." *Industrial & Engineering Chemistry Research* 62, no. 12 (2023): 5216-5229. https://doi.org/10.1021/acs.iecr.2c04150

[2] Abd, Ammar Ali, Mohd Roslee Othman, Hasan Sh Majdi, and Zuchra Helwani. "Green route for biomethane and hydrogen production via integration of biogas upgrading using pressure swing adsorption and steam-methane reforming process." *Renewable Energy* 210 (2023): 64-78. https://doi.org/10.1016/j.renene.2023.04.041

[3] Chidambaram, Arunraj, David H. Le, Jorge AR Navarro, and Kyriakos C. Stylianou. "Robust metal-organic frameworks for dry and wet biogas upgrading." *Applied Materials Today* 22 (2021): 100933. https://doi.org/10.1016/j.apmt.2020.100933

[4] Demir, Hakan, Christopher J. Cramer, and J. Ilja Siepmann. "Computational screening of metal–organic frameworks for biogas purification." *Molecular Systems Design & Engineering* 4, no. 6 (2019): 1125-1135. https://doi.org/10.1039/C9ME00095J

[5] Vilardi, Giorgio, Claudia Bassano, Paolo Deiana, and Nicola Verdone. "Exergy and energy analysis of three biogas upgrading processes." *Energy Conversion and Management* 224 (2020): 113323. https://doi.org/10.1016/j.enconman.2020.113323

[6] Glover, Joseph, and Elena Besley. "A high-throughput screening of metal–organic framework based membranes for biogas upgrading." *Faraday Discussions* 231 (2021): 235-257. https://doi.org/10.1039/D1FD00005E

[7] Emmanuel, Jwanan Luther, Mustapha Omenesa Idris, Abdulmutalib Omeiza Usman, Quasim Musa, Abdulrahman Itopa Suleiman, and Ponfa Sambo. "Biomass-Derived Activated Carbon: A Viable Material for Remediation of pb2+ and 2, 4-Dichlorophenol (2, 4 DCP) through Adsorption." *Journal of Advanced Research in Applied Sciences and Engineering Technology* 25, no. 1 (2021): 37-45. https://doi.org/10.37934/araset.25.1.3745

[8] Sahri, Dzulkarnain Mohd, Nabilah Zaini, Noor Shawal Nasri, Husna Mohd Zain, Norhana Mohamed Rashid, and Anis Shahirah Noor Shawal. "Length and Diameter Ratio Effect on Gas Homogeneity Gradients Flow for Multi-Channel Carbon Filtration System Using Computational Fluid Dynamic Analysis." *Journal of Advanced Research in Applied Mechanics* 75, no. 1 (2020): 1-5.

[9] Ghani, Nik Rashida Nik Abdul, and Mohammed Saedi Jami. "Dynamic Adsorption of Lead by Novel Graphene Oxide-polyethersulfone Nanocomposite Membrane in Fixed-bed Column." *Journal of Advanced Research in Experimental Fluid Mechanics and Heat Transfer* 2, no. 1 (2020): 1-9.

[10] Hussein, Mohd Zobir, and Rabia Baby. "Application of palm kernel shell as bio adsorbent for the treatment of heavy metal contaminated water." *Journal of Advanced Research in Applied Mechanics* 60, no. 1 (2019): 10-16.

[11] Mergenthal, Marcus, Atthasit Tawai, Suksun Amornraksa, Supacharee Roddecha, and Santi Chuetor. "Methane enrichment for biogas purification using pressure swing adsorption techniques." *Materials Today: Proceedings* 72 (2023): 2915-2920. https://doi.org/10.1016/j.matpr.2022.08.003

[12] Ismail, Marhaina, Mohamad Azmi Bustam, and Nor Ernie Fatriyah Kari. "Screening of gallate-based metal-organic frameworks for single-component CO2 and CH4 gas." In *E3S Web of Conferences*, vol. 287, p. 02005. EDP Sciences, 2021. https://doi.org/10.1051/e3sconf/202128702005

[13] Bao, Zongbi, Jiawei Wang, Zhiguo Zhang, Huabin Xing, Qiwei Yang, Yiwen Yang, Hui Wu *et al.,* "Molecular sieving of ethane from ethylene through the molecular cross-section size differentiation in gallate-based metal–organic frameworks." *Angewandte Chemie* 130, no. 49 (2018): 16252-16257. https://doi.org/10.1002/ange.201808716

[14] Ismail, Marhaina, Mohamad Azmi Bustam, Nor Ernie Fatriyah Kari, and Yin Fong Yeong. "Ideal Adsorbed Solution Theory (IAST) of Carbon Dioxide and Methane Adsorption Using Magnesium Gallate Metal-Organic Framework (Mg-gallate)." *Molecules* 28, no. 7 (2023): 3016. https://doi.org/10.3390/molecules28073016

[15] Langmuir, Irving. "The adsorption of gases on plane surfaces of glass, mica and platinum." *Journal of the American Chemical society* 40, no. 9 (1918): 1361-1403. https://doi.org/10.1021/ja02242a004

[16] Ullah, Sami, Mohamad Azmi Bustam, Mohammed Ali Assiri, Abdullah G. Al-Sehemi, Muhammad Sagir, Firas A. Abdul Kareem, Ali EI Elkhalifah, Ahmad Mukhtar, and Girma Gonfa. "Synthesis, and characterization of metal-organic frameworks-177 for static and dynamic adsorption behavior of CO2 and CH4." *Microporous and Mesoporous Materials* 288 (2019): 109569. https://doi.org/10.1016/j.micromeso.2019.109569

[17] Freundlich, H. M. F. "Over the adsorption in solution." *J. Phys. chem* 57, no. 385471 (1906): 1100-1107.

[18] Sips, R. "Combined form of Langmuir and Freundlich equations." *J. Chem. Phys* 16, no. 429 (1948): 490-495. https://doi.org/10.1063/1.1746922

[19] Guarín Romero, Jhonatan R., Juan Carlos Moreno-Piraján, and Liliana Giraldo Gutierrez. "Kinetic and equilibrium study of the adsorption of CO2 in ultramicropores of resorcinol-formaldehyde aerogels obtained in acidic and basic medium." *C* 4, no. 4 (2018): 52. https://doi.org/10.3390/c4040052

[20] Toth, J. "State equation of the solid-gas interface layers." *Acta chim. hung.* 69 (1971): 311-328.

[21] Kiełbasa, Karolina, Adrianna Kamińska, Oliwier Niedoba, and Beata Michalkiewicz. "CO2 adsorption on activated carbons prepared from molasses: A comparison of two and three parametric models." *Materials* 14, no. 23 (2021): 7458. https://doi.org/10.3390/ma14237458

[22] Mohamed, G., A. Ashraf, and A. Mohamed. "Low-Temperature Adsorption Study of Carbon Dioxide on Porous Magnetite Nanospheres Iron Oxide." (2021).

[23] Shahrom, Maisara Shahrom Raja, Cecilia Devi Wilfred, and Fai Kait Chong. "Thermodynamic and kinetic studies on CO2 capture with Poly [VBTMA][Arg]." *Journal of Physics and Chemistry of Solids* 116 (2018): 22-29. https://doi.org/10.1016/j.jpcs.2018.01.008

[24] Song, Gan, Xun Zhu, Rong Chen, Qiang Liao, Yu-Dong Ding, and Lin Chen. "An investigation of CO2 adsorption kinetics on porous magnesium oxide." *Chemical Engineering Journal* 283 (2016): 175-183. https://doi.org/10.1016/j.cej.2015.07.055

[25] Salehi, T., and D. Yousefi Kebria. "Synergy of Granular Activated Carbon and Anaerobic Mixed Culture in Phenol Bioremediation of Aqueous Solution." *Iranian (Iranica) Journal of Energy & Environment* 11, no. 3 (2020): 178-185. https://doi.org/10.5829/IJEE.2020.11.03.01

[26] Loganathan, Sravanthi, Mayur Tikmani, Satyannarayana Edubilli, Aakanksha Mishra, and Aloke Kumar Ghoshal. "CO2 adsorption kinetics on mesoporous silica under wide range of pressure and temperature." *Chemical Engineering Journal* 256 (2014): 1-8. https://doi.org/10.1016/j.cej.2014.06.091

[27] Tang, Bin, Xi Lu, Jinfeng Wang, Hao Yu, Yanchao Zhu, Steven E. Atkinson, and Xungai Wang. "Kinetic and thermodynamic studies on gas adsorption behaviour of natural fibres." *The Journal of The Textile Institute* 112, no. 9 (2021): 1390-1402. https://doi.org/10.1080/00405000.2020.1817292

[28] Raganati, Federica, Michela Alfe, Valentina Gargiulo, Riccardo Chirone, and Paola Ammendola. "Kinetic study and breakthrough analysis of the hybrid physical/chemical CO2 adsorption/desorption behavior of a magnetite-based sorbent." *Chemical Engineering Journal* 372 (2019): 526-535. https://doi.org/10.1016/j.cej.2019.04.165

[29] Naz, Saba, Abdul Rauf Khaskheli, Abdalaziz Aljabour, Huseyin Kara, Farah Naz Talpur, Syed Tufail Hussain Sherazi, Abid Ali Khaskheli, and Sana Jawaid. "Synthesis of highly stable cobalt nanomaterial using gallic acid and its application in catalysis." *Adv. Chem* 2014 (2014): 1-6. https://doi.org/10.1155/2014/686925

[30] Holder, Cameron F., and Raymond E. Schaak. "Tutorial on powder X-ray diffraction for characterizing nanoscale materials." *Acs Nano* 13, no. 7 (2019): 7359-7365. https://doi.org/10.1021/acsnano.9b05157

[31] Cui, Wen-Gang, Tong-Liang Hu, and Xian-He Bu. "Metal–organic framework materials for the separation and purification of light hydrocarbons." *Advanced Materials* 32, no. 3 (2020): 1806445. https://doi.org/10.1002/adma.201806445

[32] Shafeeyan, Mohammad Saleh, Wan Mohd Ashri Wan Daud, Amirhossein Houshmand, and Arash Arami-Niya. "Ammonia modification of activated carbon to enhance carbon dioxide adsorption: effect of pre-oxidation." *Applied Surface Science* 257, no. 9 (2011): 3936-3942. https://doi.org/10.1016/j.apsusc.2010.11.127

[33] Duan, Shuo, Min Gu, Xidong Du, and Xuefu Xian. "Adsorption equilibrium of CO2 and CH4 and their mixture on Sichuan Basin shale." *Energy & Fuels* 30, no. 3 (2016): 2248-2256. https://doi.org/10.1021/acs.energyfuels.5b02088

[34] Fernandez, David Cantador, David Suescum Morales, José Ramón Jiménez, and José María Fernández-Rodriguez. "CO_2 adsorption by organohydrotalcites at low temperatures and high pressure." *Chemical Engineering Journal* 431 (2022): 134324. https://doi.org/10.1016/j.cej.2021.134324

[35] Thommes, Matthias, Katsumi Kaneko, Alexander V. Neimark, James P. Olivier, Francisco Rodriguez-Reinoso, Jean Rouquerol, and Kenneth SW Sing. "Physisorption of gases, with special reference to the evaluation of surface area and pore size distribution (IUPAC Technical Report)." *Pure and applied chemistry* 87, no. 9-10 (2015): 1051-1069. https://doi.org/10.1515/pac-2014-1117

[36] Sotomayor, Francisco J., Katie A. Cychosz, and Matthias Thommes. "Characterization of micro/mesoporous materials by physisorption: concepts and case studies." *Acc. Mater. Surf. Res* 3, no. 2 (2018): 34-50.

[37] Wu, Yanhong, Minhua Su, Jiawei Chen, Zuopeng Xu, Jiafeng Tang, Xiangyang Chang, and Diyun Chen. "Superior adsorption of methyl orange by h-MoS2 microspheres: Isotherm, kinetics, and thermodynamic studies." *Dyes and Pigments* 170 (2019): 107591. https://doi.org/10.1016/j.dyepig.2019.107591

[38] Ursueguia, David, Eva Diaz, and Salvador Ordonez. "Adsorption of methane and nitrogen on Basolite MOFs: Equilibrium and kinetic studies." *Microporous and Mesoporous Materials* 298 (2020): 110048. https://doi.org/10.1016/j.micromeso.2020.110048